BJR

Received: 9 February 2016 | Revised: 23 April 2016 | Accepted: 19 May 2016

http://dx.doi.org/10.1259/bjr.20160140

Cite this article as:
Kim Y, Ko K, Kim D, Min C, Kim SG, Joo J, et al. Intravoxel incoherent motion diffusion-weighted MR imaging of breast cancer: association with histopathological features and subtypes. *Br J Radiol* 2016; **89**: 20160140.

FULL PAPER

Intravoxel incoherent motion diffusion-weighted MR imaging of breast cancer: association with histopathological features and subtypes

[1]YUNJU KIM, MD, [1]KYOUNGLAN KO, MD, [1]DAEHONG KIM, PhD, [2]CHANGKI MIN, BS, [3]SUNGHEON G KIM, PhD, [4]JUNGNAM JOO, PhD and [4]BORAM PARK, MS

[1]Department of Radiology, National Cancer Center, Goyang, Republic of Korea
[2]Molecular Imaging and Therapy Branch, National Cancer Center, Goyang, Republic of Korea
[3]Department of Radiology, New York University School of Medicine, New York, NY, USA
[4]Biometric Research Branch, National Cancer Center, Goyang, Republic of Korea

Address correspondence to: Dr Kyounglan Ko
E-mail: *kokrncc@gmail.com*

Objective: To evaluate the associations between intravoxel incoherent motion (IVIM)-derived parameters and histopathological features and subtypes of breast cancer.
Methods: Pre-operative MRI from 275 patients with unilateral breast cancer was analyzed. The apparent diffusion coefficient (ADC) and IVIM parameters [tissue diffusion coefficient (D_t), perfusion fraction (f_p) and pseudodiffusion coefficient] were obtained from cancer and normal tissue using diffusion-weighted imaging with *b*-values of 0, 30, 70, 100, 150, 200, 300, 400, 500 and 800 s mm^{-2}. We then compared the IVIM parameters of tumours with different histopathological features and subtypes.
Results: The ADC and D_t were lower and f_p was higher in cancers than in normal tissues ($p < 0.001$). The D_t was lower in high Ki-67 cancer than in low Ki-67 cancer ($p = 0.019$), whereas ADC showed no significant difference ($p = 0.309$). Luminal B [human epidermal growth factor receptor 2 (*HER2*)-negative] cancer showed lower ADC ($p = 0.003$) and D_t ($p = 0.001$) than other types.
Conclusion: We found low tissue diffusivity in high Ki-67 cancer and luminal B (*HER2*-negative) cancer using IVIM imaging.
Advances in knowledge: Low tissue diffusivity is more clearly shown in high Ki-67 tumours and luminal B (*HER2*-negative) tumours with the IVIM model.

INTRODUCTION

Breast cancer is a heterogeneous disease with diverse histological subtypes and clinical outcomes. There is a growing emphasis on therapeutic strategies based on intrinsic biological subtypes of breast cancer.[1,2] Gene expression profiling can be used to classify breast cancers into molecular subtypes with prognostic significance. However, because obtaining gene expression information is not always feasible, these molecular subtypes are often approximated using immunohistochemical definitions; gene amplification of oestrogen receptor (ER), progesterone receptor (PR), human epidermal growth factor receptor 2 (*HER2*) and Ki-67 labelling index. These subtypes have different patterns of disease manifestations and prognosis.[3–5]

There have been many efforts to find a correlation between tumour subtypes and imaging.[6,7] MRI is an important radiological method for the assessment of breast cancer.[8] On dynamic contrast-enhanced MRI, cancers are distinguished from normal tissues based on the alteration in vascularity and vascular permeability. By contrast, diffusion-weighted (DW) imaging provides information about microstructural properties of the tissue.[9] Increased cellularity and decreased extracellular space result in restricted diffusion in malignant tumours, observed as high signal intensity on DW images with low apparent diffusion coefficient (ADC) values. On most MRI systems, the ADC value is typically calculated with a monoexponential function.[10] In addition, microcirculatory perfusion of blood within the random capillary network can also be measured as a "pseudoperfusion" effect, commonly referred to as the intravoxel incoherent motion (IVIM).[10–12]

Since Le Bihan et al[11] proposed the concept of IVIM, a number of studies have extracted the effects of microcapillary perfusion from DW images.[10,12,13] When DW imaging is performed with multiple *b*-values (usually 0–1000 s mm^{-2} for body imaging), the signal intensity at low *b*-values (*e.g.* 0–100 s mm^{-2}) reflects both water diffusion

in tissues and microcirculation within capillaries.[10] By contrast, at higher *b*-values, the signal intensity is more reflective of tissue diffusivity. The IVIM model using a biexponential analysis provides both tissue diffusion coefficient (D_t) and pseudo-diffusion coefficient (D_p) for non-invasive assessment of the tumour microenvironment.

Recent studies have demonstrated that the IVIM model is helpful for differential diagnosis of breast lesions.[14–16] However, to the best of our knowledge, no study has reported the correlation between IVIM parameters and subtypes of breast cancer. The purpose of this study is to compare ADC and IVIM parameters [D_t, perfusion fraction (f_p) of tissues and D_p] with the histopathology and subtypes of breast tumours.

METHODS AND MATERIALS

Patients

After the receipt of institutional review board of National Cancer Center Korea approval, consecutive patients who underwent MR examination in our institution from September 2013 to December 2014 were recruited. The written informed consent was obtained from all participants. Eligible patients were identified from the prospective institutional database. The patient inclusion criteria were as follows: (a) newly diagnosed, pathologically confirmed breast cancer by needle biopsy; (b) not receiving neoadjuvant systemic treatment; (c) patient underwent surgery, *i.e.* mastectomy or breast-conserving surgery; (d) invasive cancer size of 1 cm or larger with a surgical specimen; (e) unilateral breast cancer; (f) the absence of previous interstitial mammoplasty; (g) visible solid portion of the lesion in DW imaging; and (h) grossly sufficient amount of fibroglandular tissues in the contralateral breast for comparison between tumour and normal tissue.

We identified 862 MR examinations from 824 patients during the study period (Figure 1). We excluded 549 patients: 69 patients had no malignant tumour; 11 patients had recurrent cancer and had received previous systemic or local treatment; 29 patients had undergone excisional biopsy; 140 patients received neoadjuvant systemic treatment; 9 patients were lost during the follow-up; 53 patients had ductal carcinoma *in situ* or microinvasive cancer; 74 patients had invasive cancer <1 cm in maximum diameter; 14 patients had bilateral breast cancer; 1 patient had received interstitial mammoplasty; the lesions were poorly visible in DW imaging in 128 patients; 7 patients had predominantly cystic cancer; and 14 patients had sparse fibroglandular tissues in the contralateral breast that was inadequate for comparative analysis of the normal tissue. Finally, 275 patients (all females; median age, 51 years; range, 28–83 years) were enrolled in this study.

Histopathological analysis

Histopathological reports were reviewed to determine the size, histological grade, histological type, axillary lymph node status and immunohistochemistry. Tumour size was determined as the maximum diameter of the invasive cancer. Histological grading was scored as 1–3 points according to tubule formation, pleomorphism and mitotic counts. The status of ER, PR, *HER2* gene amplification and the Ki-67 labelling index were assessed by immunohistochemistry. ER or PR positivity was defined as nuclear staining in >10% of cancer cells. For *HER2* expression, scores of 0 and 1+ were considered negative for overexpression

Figure 1. Flow diagram shows the patient selection process with exclusion criteria. DCIS, ductal carcinoma *in situ*; DW, diffusion-weighted; IVIM, intravoxel incoherent motion.

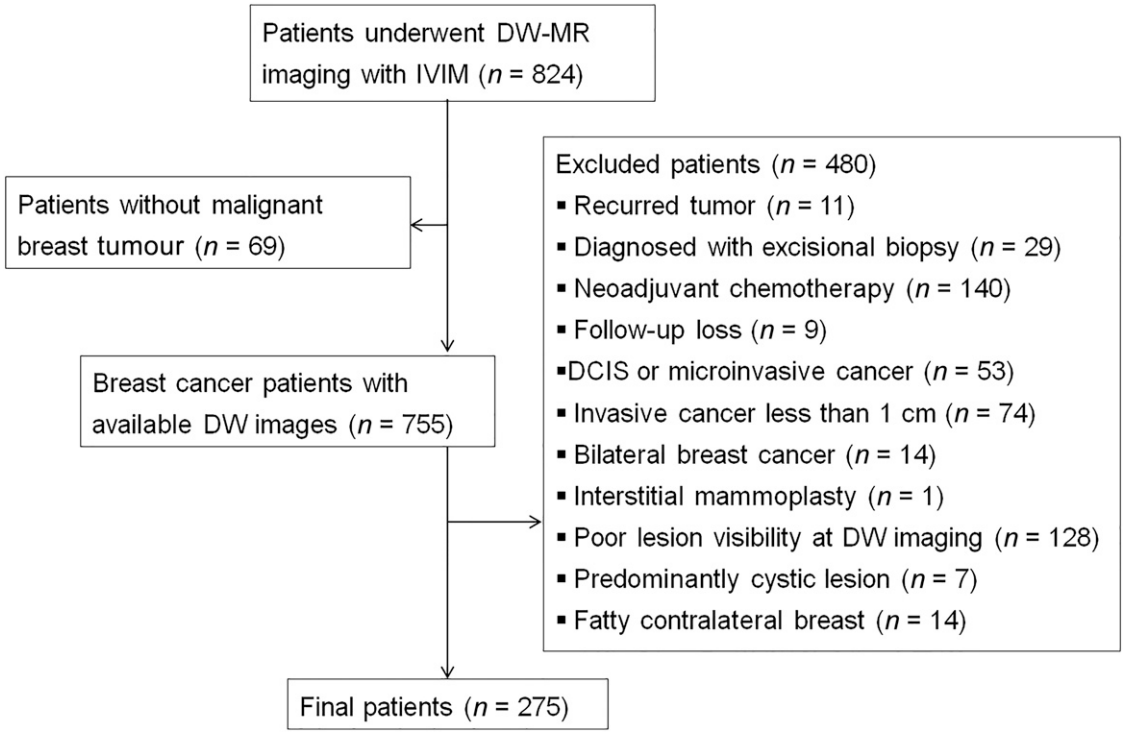

of the *HER2* gene, whereas scores of 3+ were considered positive. Gene amplification by silver *in situ* hybridization was used to determine *HER2* status in tumours with a 2+ score. Ki-67-positive cancer nuclei of 14% or greater were considered a high value.[5] Breast cancer subtypes were defined by clinicopathological criteria using surrogate markers, *i.e.* ER, PR, *HER2* and Ki-67; "luminal A": ER and/or PR positive, *HER2* negative, Ki-67 low; "luminal B (*HER2* negative)": ER and/or PR positive, *HER2* negative, Ki-67 high; "luminal B (*HER2* positive)": ER and/or PR positive, *HER2* overexpressed or amplified, any Ki-67; "*HER2* positive (non-luminal)": *HER2* over-expressed or amplified, ER and PR absent; and "triple negative (ductal)": ER and PR absent, *HER2* negative.[1]

MR protocols

MRI was performed using an Achieva® 3.0-T TX (Philips Healthcare, Eindhoven, Netherlands) with a dedicated breast surface coil and the patient in a prone position. Axial T_2 weighted images with fat-suppression [repetition time (TR)/echo time (TE), 3080/70 ms; flip angle (FA), 90°; field of view (FOV), $352 \times 352\ mm^2$; matrix size, 584×305; slice thickness, 3 mm] were obtained. Pre- and post-contrast axial T_1 weighted images (TR/TE, 4.6/2.3 ms; FA, 12°; FOV, $344 \times 344\ mm^2$; matrix size, 456×469; slice thickness, 4 mm) were obtained before and 2, 4, 6 and 8 min after an injection of $0.2\ ml\ kg^{-1}$ of body weight of gadotericacid (DOTAREM®; Guerbet, Aulnay-sous-Bois, France). After completion of dynamic contrast-enhanced imaging, axial DW images were obtained with *b*-values of 0, 30, 70, 100, 150, 200, 300, 400, 500 and 800 $s\ mm^{-2}$ by using single-shot echo-planar imaging (TR/TE, 7788/43 ms; FA, 90°; FOV, $320 \times 320\ mm^2$; matrix size, 160×166; number of excitations, 1; slice thickness, 3 mm). Total scan time for the IVIM scan was 3 min and 53 s.

Image analysis

All images were reviewed on a picture archiving and communication system workstation by a breast radiologist who was blinded to the histopathological results. DW imaging data were transferred to a personal computer for IVIM analysis using in-house software written in Interactive Data Language (Research System, Boulder, CO). A region of interest (ROI) was manually drawn on the slice with the largest tumour region enclosing the entire lesion. A ROI was drawn on DW images, using T_2 weighted and contrast-enhanced T_1 weighted sequences as references for ROI demarcation. In case of multiple malignancies in a breast, only the largest lesion was selected. Grossly cystic or necrotic portions were avoided. A region of normal fibroglandular tissue was sampled in the contralateral breast. The normal tissue ROI was usually drawn in the symmetric area of the lesion at the same slice while avoiding gross fat. If sufficient normal tissue was not available, the closest region was selected.

For the conventional analysis, the ADC was calculated with a monoexponential decay function:

$$S = S_0\, e^{-b\mathrm{ADC}}$$

For the IVIM analysis, a two-compartmental model of DW signal intensity is described by the following biexponential function:[12]

$$S = S_0\left[\left(1 - f_p\right)e^{-bD_t} + f_p e^{-bD_p}\right]$$

where S_0 is the DW MR image acquired without diffusion-weighting ($b = 0\ s\ mm^{-2}$). Typically, the D_p is significantly greater than the D_t, and its influence on DW signals is weak when *b*-values are large enough. Therefore, the D_t can be calculated from data with higher *b*-values ($b > 200\ s\ mm^{-2}$):[13,16]

Table 1. Study population and histopathological features

Characteristic	Value
Age (years)	51.0 (28–83)
Size of invasive cancer (cm)	2.0 (1–6.2)
Histological grade	
1	17 (6.2)
2	127 (46.2)
3	131 (47.6)
Histological type	
Invasive ductal carcinoma	228 (82.9)
Non-invasive ductal carcinoma	47 (17.1)
Nodal status	
Negative	190 (69.1)
Positive	85 (30.9)
Oestrogen receptor	
Negative	81 (29.5)
Positive	194 (70.5)
Progesterone receptor	
Negative	103 (37.5)
Positive	172 (62.5)
HER2 overexpression	
Negative	218 (79.3)
Positive	57 (20.7)
Ki-67 labelling index	27 (1–95)
<14%	61 (22.2)
≥14%	214 (77.8)
Subtype	
Luminal A	58 (21.1)
Luminal B (*HER2* negative)	108 (39.3)
Luminal B (*HER2* positive)	30 (10.9)
HER2 positive (non-luminal)	27 (9.8)
Triple negative (ductal)	52 (18.9)

HER2, human epidermal growth factor receptor 2.
Data are presented as the median (range) or *n* (%).

$$S_{high} = S_0\left(1 - f_p\right)e^{-bD_t}$$

assuming that the perfusion effect is negligible. The f_p can be determined using the zero intercept S_{high} ($b = 0$) along with the unweighted ($b = 0\,s\,mm^{-2}$) signal S_0 according to:

$$f_p = \frac{S_0 - S_{high}(b=0)}{S_0}$$

Finally, the D_p can be calculated by a partially constrained non-linear fit of the entire data set using D_t and f_p. Estimation of the above parameters was performed by minimizing the sum of square differences between the above signal model and the measurement data using the Simplex algorithm.

Statistical analysis

Statistical analyses were performed using SPSS® software v. 22 (IBM Corp., New York, NY; formerly SPSS Inc., Chicago, IL). Wilcoxon signed-rank tests were used for comparisons between the cancer and normal tissue in each patient. Tumours were assigned to one of two groups according to histopathology: Tumour size (≤2 *vs* >2 cm), histological grade (grades 1 and 2 *vs* 3), histological type [invasive ductal carcinoma (IDC) *vs* non-IDC], axillary nodal metastasis (negative *vs* positive), and expression status of ER (negative *vs* positive), PR (negative *vs* positive), *HER2* (negative *vs* positive) and Ki-67 (<14% *vs* ≥14%). For analysis of histopathological features and subtypes, Mann–Whitney *U* tests and Kruskall–Wallis tests were used. *p*-values <0.05 were considered statistically significant.

RESULTS

Patients and histopathology

All 275 patients underwent mastectomy ($n = 40$, 14.5%) or breast-conserving surgery ($n = 235$, 85.5%) with axillary dissection or sentinel lymph node biopsy. Table 1 summarizes the histopathological data after surgery. The median size of invasive cancer was 2.0 cm (range 1.0–6.2 cm). Histological grades were as follows: 17 tumours of grade 1 (6.2%), 127 tumours of grade 2 (46.2%) and 131 tumours of grade 3 (47.6%). Histological types were as follows: 228 (82.9%) IDCs, 13 (4.7%) invasive lobular carcinomas, 13 (4.7%) invasive cribriform carcinomas, 7 (2.5%) metaplastic carcinomas, 7 (2.5%) mucinous carcinomas, 2 (0.7%) invasive micropapillary carcinomas, 2 (0.7%) mixed ductal and lobular carcinomas, 2 (0.7%) mixed metaplastic and ductal carcinomas and 1 (0.4%) invasive micropapillary carcinoma. 85 (30.9%) patients had axillary lymph node metastasis and 190 (69.1%) did not. No patients had distant metastasis. Immunohistochemistry showed ER positivity in 194 (70.5%), PR positivity in 172 (62.5%), *HER2* positivity in 57 (20.7%) and high Ki-67 (≥14%) in 214 (77.8%) patients. The median value of Ki-67 was 27 (range 1–95). Tumour subtype was categorized as luminal A in 58 (21.1%), luminal B (*HER2* negative) in 108 (39.3%), luminal B (*HER2* positive) in 30 (10.9%), *HER2* positive (non-luminal) in 27 (9.8%) and triple negative (ductal) in 52 (18.9%) patients.

Intravoxel incoherent motion parameters in breast cancer and normal tissue

Table 2 shows a comparison of ADC and IVIM parameters between cancer and normal tissue. The ADC and D_t of cancers were significantly lower than those of normal tissue ($p < 0.001$). The f_p was higher in cancers than in normal tissue ($p < 0.001$). There was no significant difference in D_p between cancers and normal tissue ($p = 0.199$).

Histopathological features and subtypes

Table 3 shows a comparison of ADC and IVIM parameters with regard to histopathological features. Larger tumours had higher f_p and D_p than smaller tumours ($p = 0.048$ and $p = 0.038$). The D_p was higher in high-grade tumours than in low-grade tumours ($p = 0.001$). There was no significant difference in ADC and IVIM parameters between IDC and non-IDC tumours. Patients with metastatic axillary lymph nodes showed higher values of ADC and f_p compared with patients without metastatic axillary lymph nodes ($p = 0.005$ and $p = 0.035$). The D_p was higher in negative ER or PR groups than positive groups ($p = 0.008$ and $p = 0.001$). There were no significant differences in ADC and IVIM parameters correlating with *HER2* positivity. D_t was lower in the high Ki-67 group than in the low Ki-67 group ($p = 0.019$), whereas the ADC showed no significant differences ($p = 0.309$). However, there was no statistical significance between Ki-67 and DW imaging parameters in the Spearman correlation analysis.

Table 4 shows a comparison of ADC and IVIM parameters with regard to tumour subtypes. Luminal A cancer showed higher D_t

Table 2. Comparison of apparent diffusion coefficient (ADC) and intravoxel incoherent motion parameters in breast cancer and normal tissue

Parameter	Cancer	Normal tissue	*p*-value
ADC ($\times 10^{-3}\,mm^2\,s^{-1}$)	1.18 (0.72–1.99)	1.64 (1.02–2.60)	<0.001
D_t ($\times 10^{-3}\,mm^2\,s^{-1}$)	0.90 (0.21–1.77)	1.45 (0.82–2.61)	<0.001
f_p (%)	11.87 (4.83–42.42)	8.35 (1.05–21.71)	<0.001
D_p ($\times 10^{-3}\,mm^2\,s^{-1}$)	13.89 (2.12–72.91)	14.45 (4.57–99.08)	0.199

D_p, pseudodiffusion coefficient; D_t, tissue diffusion coefficient; f_p, perfusion fraction.
Data are presented as the median (range).
p-values for differences were determined by Wilcoxon signed-rank test.

Table 3. Apparent diffusion coefficient (ADC) and intravoxel incoherent motion parameters with regard to histopathological features

Variable		*n*	ADC ($\times 10^{-3}$ mm^2 s^{-1})	*p*-value	D_t ($\times 10^{-3}$ mm^2 s^{-1})	*p*-value	f_p (%)	*p*-value	D_p ($\times 10^{-3}$ mm^2 s^{-1})	*p*-value
Tumour size (cm)	≤2	150	1.15 (0.76–1.91)	0.093	0.91 (0.21–1.65)	0.671	11.27 (5.32–42.42)	0.048	12.49 (2.12–72.91)	0.038
	>2	125	1.18 (0.72–0.99)		0.90 (0.35–1.77)		12.25 (4.83–28.81)		15.95 (4.10–48.82)	
Histological grade	1 or 2	144	1.16 (0.72–1.99)	0.599	0.89 (0.21–1.77)	0.979	11.89 (5.86–42.42)	0.829	11.91 (2.12–72.91)	0.001
	3	131	1.18 (0.81–1.91)		0.91 (0.54–1.44)		11.84 (4.83–27.22)		16.92 (4.83–60.98)	
Histological type	IDC	228	1.17 (0.72–1.86)	0.876	0.90 (0.21–1.44)	0.882	11.83 (5.32–42.42)	0.564	13.85 (2.12–72.91)	0.428
	Non-IDC	47	1.18 (0.76–1.99)		0.91 (0.43–1.77)		11.97 (4.83–25.04)		14.15 (4.10–39.59)	
Axillary LN metastasis	Negative	190	1.15 (0.76–1.99)	0.005	0.89 (0.21–1.77)	0.327	11.72 (4.83–28.34)	0.035	13.37 (2.12–63.04)	0.433
	Positive	85	1.21 (0.72–1.86)		0.92 (0.35–1.43)		12.11 (6.17–42.42)		15.45 (4.10–72.91)	
ER	Negative	81	1.23 (0.82–1.76)	0.130	0.91 (0.60–1.44)	0.610	11.93 (4.83–23.73)	0.738	17.82 (4.83–60.98)	0.008
	Positive	194	1.16 (0.72–1.99)		0.89 (0.21–1.77)		11.84 (5.32–42.42)		12.50 (2.12–72.91)	
PR	Negative	103	1.24 (0.82–1.76)	0.013	0.94 (0.60–1.44)	0.169	12.11 (4.83–28.81)	0.663	17.82 (4.83–60.98)	0.001
	Positive	172	1.14 (0.72–1.99)		0.88 (0.21–1.77)		11.75 (5.32–42.42)		11.91 (2.12–72.91)	
HER2	Negative	218	1.17 (0.72–1.99)	0.071	0.89 (0.21–1.77)	0.109	11.89 (4.83–42.42)	0.448	13.08 (2.12–72.91)	0.082
	Positive	57	1.25 (0.81–1.91)		0.93 (0.60–1.36)		11.51 (5.86–28.81)		16.36 (6.68–39.59)	
Ki-67	<14%	61	1.20 (0.80–1.99)	0.309	0.97 (0.43–1.77)	0.019	11.23 (6.39–19.45)	0.080	11.61 (4.10–52.01)	0.015
	≥14%	214	1.17 (0.72–1.91)		0.88 (0.21–1.65)		12.00 (4.83–42.42)		14.78 (2.12–72.91)	

D_p, pseudodiffusion coefficient; D_t, tissue diffusion coefficient; ER, oestrogen receptor; f_p, perfusion fraction; *HER2*, human epidermal growth factor receptor 2; IDC, invasive ductal carcinoma; LN, lymph node; PR, progesterone receptor.
Data are presented as the median (range).
p-values for differences were determined by Mann–Whitney *U* test.

Table 4. Apparent diffusion coefficient (ADC) and intravoxel incoherent motion parameters with regard to subtypes

Subtype	*n*	ADC ($\times 10^{-3}$ mm^2 s^{-1})	*p*-value	D_t ($\times 10^{-3}$ mm^2 s^{-1})	*p*-value	f_p (%)	*p*-value	D_p ($\times 10^{-3}$ mm^2 s^{-1})	*p*-value
Luminal A	58	1.21 (0.80–1.99)	0.047	0.97 (0.43–1.77)	0.011	11.15 (6.39–19.45)	0.187	11.62 (4.10–52.01)	0.018
Luminal B (*HER2* negative)	108	1.13 (0.72–1.83)		0.86 (0.21–1.65)		12.23 (5.32–42.42)		13.44 (2.12–72.91)	
Luminal B (*HER2* positive)	30	1.23 (0.81–1.91)		0.95 (0.66–1.36)		10.72 (5.86–28.81)		12.67 (6.68–39.59)	
HER2 positive (non-luminal)	27	1.26 (0.94–1.68)		0.91 (0.60–1.18)		12.57 (8.36–23.73)		19.39 (8.17–36.92)	
Triple negative (ductal)	52	1.21 (0.82–1.76)		0.92 (0.60–1.44)		11.92 (4.83–21.03)		17.26 (4.83–60.98)	

D_p, pseudodiffusion coefficient; D_t, tissue diffusion coefficient; f_p, perfusion fraction; *HER2*, human epidermal growth factor receptor 2.
Data are presented as the median (range).
p-values for differences were determined by Kruskall–Wallis test.

and lower D_p than other types ($p = 0.031$ and $p = 0.018$) (Figure 2). The ADC and f_p were not different in luminal A cancer compared with other types ($p = 0.339$ and $p = 0.067$). Luminal B (*HER2*-negative) cancer showed lower ADC and D_t than other types ($p = 0.003$ and $p = 0.001$) (Figure 3). *HER2*-positive cancer showed higher D_p than other types ($p = 0.007$). Luminal B (*HER2*-positive) and triple-negative cancers showed no significant differences compared with other types. A comparison of luminal B (*HER2* negative) and luminal A showed lower ADC and D_t and higher f_p in luminal B (*HER2*-negative) tumours ($p = 0.044$, $p = 0.003$ and $p = 0.036$, respectively). The D_p was not different between these two groups.

DISCUSSION

This study demonstrated that ADC and IVIM parameters differ according to histopathological features and subtypes of breast cancer. Luminal B (*HER2*-negative) cancer showed lower ADC and D_t than other types. The difference was more significant in D_t than ADC. On the other hand, luminal A cancer showed higher D_t than other types. High Ki-67 cancers showed lower D_t than low Ki-67 tumours, whereas ADC was not significantly different.

In a study of 86 patients with luminal-type invasive breast cancer, ADC values showed a negative correlation with Ki-67.[17] The authors performed conventional measurements of the mean ADCs by ROI and histogram analysis of the entire tumour volume. They concluded that the mean ADC would be useful for assessing Ki-67. This correlation was also demonstrated in a study of meningioma grading.[18] There was a significant inverse correlation between ADC and Ki-67 for low-grade and aggressive meningiomas. Such correlation can be expected, as a higher cell proliferation indicated by a high Ki-67 expression level can lead to a higher cell density indicated by a lower ADC value. However, this relationship is not always observed in tumours of which cell density can also be affected by other factors, such as necrosis. Another possibility is that the ADC measurement can be compromised by the perfusion effect. De Felice et al[19] reported that there was no statistically significant correlation between ADC values and Ki-67 in their breast cancer study. Our results show that D_t provides a better estimate of Ki-67 than ADC values, suggesting that D_t may be a better measure to assess the cell density and/or proliferation status.

Mazurowski et al[7] performed radiogenomic analysis of breast cancer. After extracting 23 MRI features from the lesions, they evaluated the associations between imaging features and molecular subtypes based on genomic data. They found that the luminal B subtype was associated with enhancement features. A large differential was revealed between the rate of enhancement of luminal B cancer and normal background parenchyma. Grimm et al[20] analyzed the association between MRI features and molecular subtypes determined by surrogate markers. While imaging features were associated with luminal A and luminal B subtypes, no association was found for other types. It is notable that extracted image features can be correlated to molecular subtypes, particularly for luminal B cancers.

Figure 2. Magnetic resonance images of a 46-year-old female with luminal A type invasive ductal carcinoma in the left breast. The malignant mass is shown in (a) a contrast-enhanced T_1 weighted image, (b) a diffusion-weighted image ($b = 800\ s\ mm^{-2}$) and (c) an apparent diffusion coefficient map. (d) The graph shows the biexponential signal decay depending on the *b*-value.

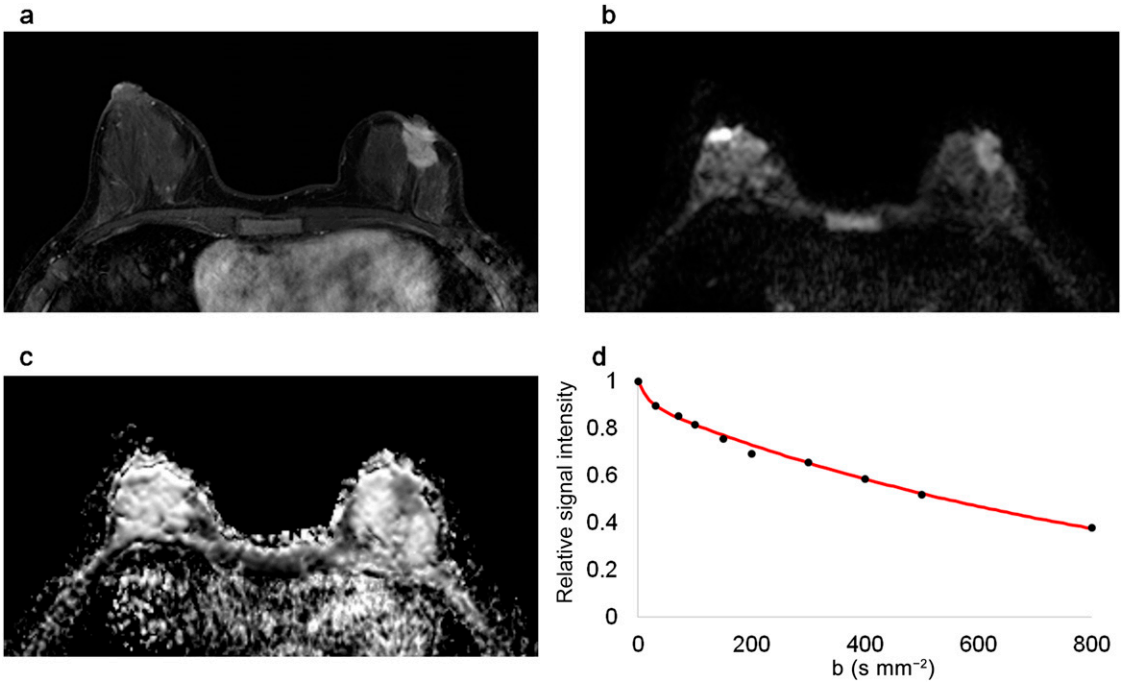

Recent studies based on gene expression profiling demonstrated that luminal A and luminal B breast cancers are distinct entities, with specific oncogenic drivers.[4] Luminal B cancers have a worse prognosis and a distinctive response to systemic therapy than luminal A cancers. Practically, luminal B cancers are differentiated from luminal A cancers based on proliferation markers.[4,5]

Figure 3. MR images of a 41-year-old female with luminal B (human epidermal growth factor receptor 2-negative) type invasive ductal carcinoma in the right breast. The malignant mass is demonstrated in (a) a contrast-enhanced T_1 weighted image and (b) a diffusion-weighted image ($b = 800\ s\ mm^{-2}$). (c) The signal intensity of the tumour decays quickly at low *b*-values. (d) The signal intensity decay of the normal tissue is relatively flat at low *b*-values.

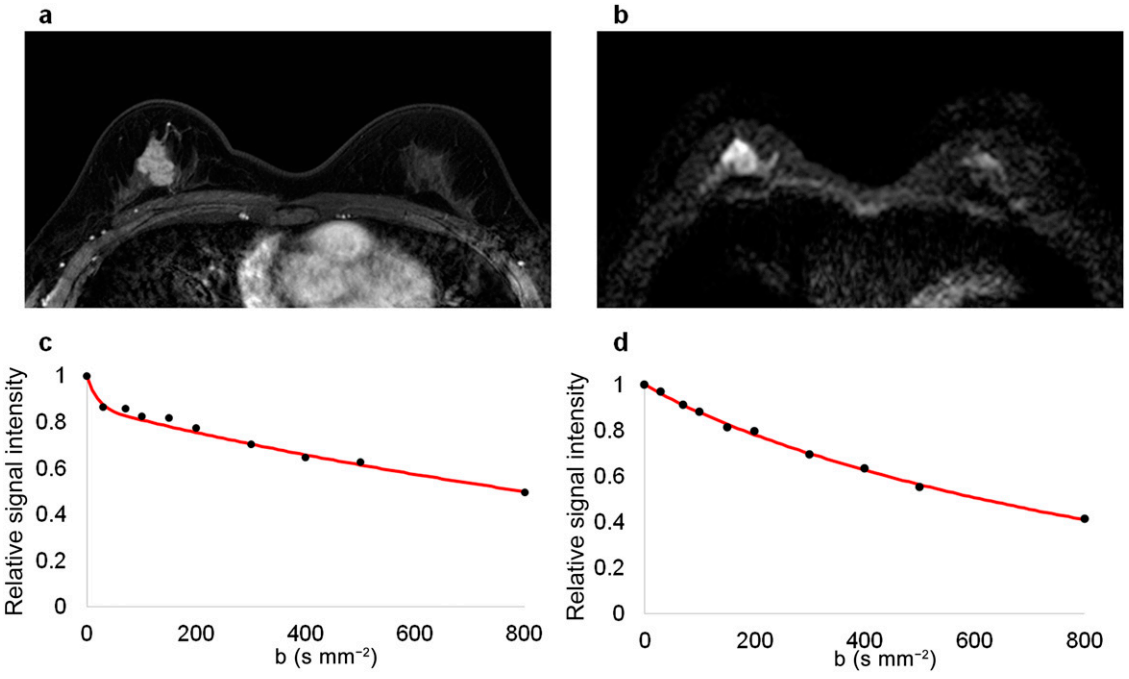

Although tumour grade is widely used for assessing proliferation status, considerable interobserver discrepancies have been reported for grading.[21] Ki-67 is a well-established cell proliferation marker in cancer.[5] Although it is an excellent surrogate biomarker for luminal B cancers, there is a controversy about the cut-off value.[1,2]

The median ADC and D_t ($\times 10^{-3}$ mm^2 s^{-1}) of tumours (1.18 and 0.90) were significantly lower than those of normal tissue (1.64 and 1.45) ($p < 0.001$). There was a larger difference between ADC and D_t in cancer than in normal tissue. Previous studies have shown that perfusion effects were small in DW images of normal breast tissue.[14–16] Mean ADC and D_t ($\times 10^{-3}$ mm^2 s^{-1}) ranged from 0.95 to 1.40 and 0.85–1.29 in cancer, respectively, and ranged from 2.01 to 2.44 and 1.96–2.36 in normal tissue. Each study used several *b*-values ranging from 0 to 1000 s mm^{-2}. Although our results from tumour tissue correspond with those studies, our results from normal tissue show generally lower values. Meanwhile, a close relationship might be expected between perfusion indexes derived from IVIM and perfusion parameters derived using contrast medium. However, this relationship is controversial, possibly because perfusion parameters derived from IVIM may comprise more than one physiological process.[10] Our study showed higher f_p in cancers than in normal tissue ($p < 0.001$). This tendency corresponds with previous studies, although the specific values vary between studies.[14,15] The f_p was also higher in larger tumours or tumours with axillary metastasis. Luminal B (*HER2*-negative) tumours showed higher f_p than luminal A.

There was no significant difference in D_p between cancer and normal tissue ($p = 0.199$). However, Liu et al[15] reported that the D_p of cancer was significantly smaller than that of normal tissue. Their results for ADC, D_t and f_p differences between cancer and normal tissue are similar to our own. D_p values were not available in normal tissue in other studies.[14,16] In comparisons of histopathological features, the D_p was higher in large tumours, high-grade tumours or hormone receptor-negative tumours. Further investigations are needed to explain the perfusion parameters derived from IVIM.

The lack of standardization is one of the major challenges in adopting DW imaging for tumour assessment.[22] To avoid the potential effects of contrast media, it was recommended to perform DW imaging prior to administration of the contrast agent.[23] However, as it takes a relatively long time to acquire breast MR images, some patients move their bodies over time. For the more practical purpose, our institution acquired DW images after the routine post-contrast T_1 weighted series during the study period. In a meta-analysis on the 1.5-T breast DW imaging, Dorrius et al[24] concluded that ADC is not significantly affected by the contrast medium prior to DW imaging. There was some literature about the effect of contrast agent at the abdominal DW imaging.[25–27] Choi et al[25] reported that ADCs of focal hepatic lesions were not significantly changed after administration of gadoxetic acid disodium, whereas ADCs of the liver were significantly decreased. On the other hand, Chiu et al[26] demonstrated that the ADCs of focal hepatic lesions and liver tended to decrease after administration of gadolinium-diethylenetriaminepenta-acetic acid, although they did not reach statistical significance. Wang et al[27] reported that intravenous gadolinium administration does not make a significant difference in ADCs of the liver, spleen or pancreas, whereas the values were decreased after contrast enhancement in the kidneys. As mentioned earlier, ADC and D_t of the normal tissue were generally lower in our study, comparing to previous studies. Further studies are warranted to assess the effect of the contrast medium on DW-derived parameters of breast MRI.

This study has other limitations. First, a selection bias may exist. Because we excluded patients who received neoadjuvant systemic treatment, relatively advanced cancers were not included. Many cases, including non-mass enhancement, were excluded because of poor visibility on DW imaging. Second, in this study, subtypes were defined immunohistochemically using surrogate markers. Although this classification is widely accepted for practical purposes, gene expression array information is preferred as a basis for chemotherapy decisions.[1,2] Third, a ROI was selected on one representative slice using conventional methods, not encompassing the entire tumour volume. Mori et al[17] suggested that the mean ADC using a conventional method is practical for assessing Ki-67 in luminal breast cancer.

As multigene molecular assays have become feasible, therapeutic strategies have been changing. Along with these changes, there have been many attempts to introduce more sophisticated methods in the field of cancer imaging. In conclusion, with the IVIM model, low tissue diffusivity was more clearly shown in high Ki-67 tumours and luminal B (*HER2*-negative) tumours. Further research is needed to confirm imaging–pathology correlations based on gene profiling.

REFERENCES

1. Goldhirsch A, Wood WC, Coates AS, Gelber RD, Thurlimann B, Senn HJ, et al. Strategies for subtypes—dealing with the diversity of breast cancer: highlights of the St. Gallen International Expert Consensus on the Primary Therapy of Early Breast Cancer 2011. *Ann Oncol* 2011; **22**: 1736–47. doi: http://dx.doi.org/10.1093/annonc/mdr304
2. Goldhirsch A, Winer EP, Coates AS, Gelber RD, Piccart-Gebhart M, Thurlimann B, et al. Personalizing the treatment of women with early breast cancer: highlights of the St Gallen International Expert Consensus on the Primary Therapy of Early Breast Cancer 2013. *Ann Oncol* 2013; **24**: 2206–23. doi: http://dx.doi.org/10.1093/annonc/mdt303
3. Voduc KD, Cheang MC, Tyldesley S, Gelmon K, Nielsen TO, Kennecke H. Breast cancer subtypes and the risk of local and regional relapse. *J Clin Oncol* 2010; **28**: 1684–91. doi: http://dx.doi.org/10.1200/jco.2009.24.9284
4. Ades F, Zardavas D, Bozovic-Spasojevic I, Pugliano L, Fumagalli D, de Azambuja E, et al. Luminal B breast cancer: molecular

characterization, clinical management, and future perspectives. *J Clin Oncol* 2014; **32**: 2794–803. doi: http://dx.doi.org/10.1200/jco.2013.54.1870
5. Cheang MC, Chia SK, Voduc D, Gao D, Leung S, Snider J, et al. Ki67 index, HER2 status, and prognosis of patients with luminal B breast cancer. *J Natl Cancer Inst* 2009; **101**: 736–50. doi: http://dx.doi.org/10.1093/jnci/djp082
6. Boisserie-Lacroix M, Hurtevent-Labrot G, Ferron S, Lippa N, Bonnefoi H, Mac Grogan G. Correlation between imaging and molecular classification of breast cancers. *Diagn Interv Imaging* 2013; **94**: 1069–80. doi: http://dx.doi.org/10.1016/j.diii.2013.04.010
7. Mazurowski MA, Zhang J, Grimm LJ, Yoon SC, Silber JI. Radiogenomic analysis of breast cancer: luminal B molecular subtype is associated with enhancement dynamics at MR imaging. *Radiology* 2014; **273**: 365–72. doi: http://dx.doi.org/10.1148/radiol.14132641
8. Brandao AC, Lehman CD, Partridge SC. Breast magnetic resonance imaging: diffusion-weighted imaging. *Magn Reson Imaging Clin N Am* 2013; **21**: 321–36. doi: http://dx.doi.org/10.1016/j.mric.2013.01.002
9. Malayeri AA, El Khouli RH, Zaheer A, Jacobs MA, Corona-Villalobos CP, Kamel IR, et al. Principles and applications of diffusion-weighted imaging in cancer detection, staging, and treatment follow-up. *Radiographics* 2011; **31**: 1773–91. doi: http://dx.doi.org/10.1148/rg.316115515
10. Koh DM, Collins DJ, Orton MR. Intravoxel incoherent motion in body diffusion-weighted MRI: reality and challenges. *AJR Am J Roentgenol* 2011; **196**: 1351–61. doi: http://dx.doi.org/10.2214/ajr.10.5515
11. Le Bihan D, Breton E, Lallemand D, Grenier P, Cabanis E, Laval-Jeantet M. MR imaging of intravoxel incoherent motions: application to diffusion and perfusion in neurologic disorders. *Radiology* 1986; **161**: 401–7. doi: http://dx.doi.org/10.1148/radiology.161.2.3763909
12. Le Bihan D, Breton E, Lallemand D, Aubin ML, Vignaud J, Laval-Jeantet M. Separation of diffusion and perfusion in intravoxel incoherent motion MR imaging. *Radiology* 1988; **168**: 497–505. doi: http://dx.doi.org/10.1148/radiology.168.2.3393671
13. Suo S, Lin N, Wang H, Zhang L, Wang R, Zhang S, et al. Intravoxel incoherent motion diffusion-weighted MR imaging of breast cancer at 3.0 tesla: comparison of different curve-fitting methods. *J Magn Reson Imaging* 2015; **42**: 362–70. doi: http://dx.doi.org/10.1002/jmri.24799
14. Bokacheva L, Kaplan JB, Giri DD, Patil S, Gnanasigamani M, Nyman CG, et al. Intravoxel incoherent motion diffusion-weighted MRI at 3.0 T differentiates malignant breast lesions from benign lesions and breast parenchyma. *J Magn Reson Imaging* 2014; **40**: 813–23. doi: http://dx.doi.org/10.1002/jmri.24462
15. Liu C, Liang C, Liu Z, Zhang S, Huang B. Intravoxel incoherent motion (IVIM) in evaluation of breast lesions: comparison with conventional DWI. *Eur J Radiol* 2013; **82**: e782–9. doi: http://dx.doi.org/10.1016/j.ejrad.2013.08.006
16. Sigmund EE, Cho GY, Kim S, Finn M, Moccaldi M, Jensen JH, et al. Intravoxel incoherent motion imaging of tumor microenvironment in locally advanced breast cancer. *Magn Reson Med* 2011; **65**: 1437–47. doi: http://dx.doi.org/10.1002/mrm.22740
17. Mori N, Ota H, Mugikura S, Takasawa C, Ishida T, Watanabe G, et al. Luminal-type breast cancer: correlation of apparent diffusion coefficients with the Ki-67 labeling index. *Radiology* 2015; **274**: 66–73. doi: http://dx.doi.org/10.1148/radiol.14140283
18. Tang Y, Dundamadappa SK, Thangasamy S, Flood T, Moser R, Smith T, et al. Correlation of apparent diffusion coefficient with Ki-67 proliferation index in grading meningioma. *AJR Am J Roentgenol* 2014; **202**: 1303–8. doi: http://dx.doi.org/10.2214/ajr.13.11637
19. De Felice C, Cipolla V, Guerrieri D, Santucci D, Musella A, Porfiri LM, et al. Apparent diffusion coefficient on 3.0 tesla magnetic resonance imaging and prognostic factors in breast cancer. *Eur J Gynaecol Oncol* 2014; **35**: 408–14.
20. Grimm LJ, Zhang J, Mazurowski MA. Computational approach to radiogenomics of breast cancer: luminal A and luminal B molecular subtypes are associated with imaging features on routine breast MRI extracted using computer vision algorithms. *J Magn Reson Imaging* 2015; **42**: 902–7. doi: http://dx.doi.org/10.1002/jmri.24879
21. Paik S, Shak S, Tang G, Kim C, Baker J, Cronin M, et al. A multigene assay to predict recurrence of tamoxifen-treated, node-negative breast cancer. *N Engl J Med* 2004; **351**: 2817–26. doi: http://dx.doi.org/10.1056/NEJMoa041588
22. Koh DM, Collins DJ. Diffusion-weighted MRI in the body: applications and challenges in oncology. *AJR Am J Roentgenol* 2007; **188**: 1622–35. doi: http://dx.doi.org/10.2214/ajr.06.1403
23. Woodhams R, Ramadan S, Stanwell P, Sakamoto S, Hata H, Ozaki M, et al. Diffusion-weighted imaging of the breast: principles and clinical applications. *Radiographics* 2011; **31**: 1059–84. doi: http://dx.doi.org/10.1148/rg.314105160
24. Dorrius MD, Dijkstra H, Oudkerk M, Sijens PE. Effect of *b*-value and pre-admission of contrast on diagnostic accuracy of 1.5-T breast DWI: a systematic review and meta-analysis. *Eur Radiol* 2014; **24**: 2835–47. doi: http://dx.doi.org/10.1007/s00330-014-3338-z
25. Choi JS, Kim MJ, Choi JY, Park MS, Lim JS, Kim KW. Diffusion-weighted MR imaging of liver on 3.0-Tesla system: effect of intravenous administration of gadoxetic acid disodium. *Eur Radiol* 2010; **20**: 1052–60. doi: http://dx.doi.org/10.1007/s00330-009-1651-8
26. Chiu FY, Jao JC, Chen CY, Liu GC, Jaw TS, Chiou YY, et al. Effect of intravenous gadolinium-DTPA on diffusion-weighted magnetic resonance images for evaluation of focal hepatic lesions. *J Comput Assist Tomogr* 2005; **29**: 176–80. doi: http://dx.doi.org/10.1097/01.rct.0000157472.98277.5c
27. Wang CL, Chea YW, Boll DT, Samei E, Neville AM, Dale BM, et al. Effect of gadolinium chelate contrast agents on diffusion weighted MR imaging of the liver, spleen, pancreas and kidney at 3 T. *Eur J Radiol* 2011; **80**: e1–7. doi: http://dx.doi.org/10.1016/j.ejrad.2010.05.019